Variants and Pitfalls of PET/CT in Neuroendocrine Tumors

Alessio Imperiale, Leah Meuter, Karel Pacak, David Taïeb

Version of Record: https://www.sciencedirect.com/science/article/pii/S0001299821000143
Manuscript_17662b8f18653e6d3a4b7d95adc96ead

Variants and pitfalls of PET/CT in neuroendocrine tumors

Alessio Imperiale[1], Leah Meuter[2], Karel Pacak[2], David Taïeb[3]

[1]Department of Nuclear Medicine and Molecular Imaging – Institut de Cancérologie de Strasbourg Europe (ICANS), IPHC, UMR 7178, CNRS/University of Strasbourg, France
[2]Section on Medical Neuroendocrinology, *Eunice Kennedy Shriver* National Institute of Child Health and Human Development, National Institutes of Health, Bethesda, USA
[3]Department of Nuclear Medicine, La Timone University Hospital, CERIMED, Aix-Marseille University, France

Abstract

Management of patients with neuroendocrine neoplasms (NEN) is complex and warrants referral of these patients to high volume centers with appropriate expertise to ensure favorable outcomes. PET/CT becomes increasingly important in every step of their management and outcome. The choice of radiopharmaceutical heavily depends on tumor origin, which is intimately interconnected to embryology, grade and clinical presentation (e.g., diagnostic vs theranostic settings). The aim of this review is to describe the role of SSTR, ^{18}F-FDOPA, and ^{18}F-FDG PET imaging in the evaluation of NEN patients. There is emphasis on the main variants, caveats, and pitfalls that can be observed within these modalities. Nuclear physicians must be equipped with the skills to handle potential variants, caveats, and pitfalls that are commonly encountered in NEN imaging, and they should understand the expected imaging features that are encountered across various types of NENs.

Indications of PET/CT

Patients with neuroendocrine neoplasms (NEN) present in widely variable ways, in which imaging plays an important role. NENs are a heterogeneous group of neoplasms such as pancreatic NEN, small intestine (SI-NEN), lung NEN, medullary thyroid carcinoma (MTC), pheochromocytoma, and paraganglioma. There have been many consensus or near consensus made by expert panels that have proposed recommendations regarding PET/CT indications for these tumors (i.e., European Association of Nuclear Medicine, Society of Nuclear Medicine and Molecular Imaging, American Thyroid Association, European Neuroendocrine Tumor Society, European Society for Medical Oncology**,** Joint international consensus statements**,** North American Neuroendocrine Tumor Society and guidelines from various national societies).[1-9]

Table 1 summarizes endoscopic investigations and morphological imaging according to different clinical scenarios. PET/CT can complement these investigations and may guide the proper clinical management on almost every level of any patient.

PET/CT is currently indicated in well-differentiated GEP-NEN (staging, restaging), insulinoma, ectopic Cushing syndrome, MTC, pheochromocytoma (PHEO), paraganglioma (PGL), and patients with an unknown primary tumor.

Table 1. Endoscopic investigations and morphological imaging according to different NEN

	Primary	Loco-regional	Distant
Pancreas	CT, MRI, endoscopy (EUS)	CT/MRI	
Small intestine	CT (CT enteroclysis) DB enteroscopy (unknown primary)	CT	
Duodenum	EUS, duodenoscopy	CT	
Colon	Colonoscopy, CT	CT	CT, MRI for liver, bone (selected cases) and brain (selected cases)
Rectum	Rectoscopy, EUS, CT		
Bronchial	Bronchoscopy, CT	CT	
MTC	Neck US	Neck US, CT	
PHEO/PGL	CT/MRI	CT/MRI	

CT: Computed Tomography
MRI: Magnetic resonance imaging
US: Ultrasound
DB: Double balloon
EUS: Endoscopic ultrasound

Choice of the optimal radiopharmaceutical

The decision to use a particular radiopharmaceutical depends heavily on tumor origin, which is closely related to developmental features, tumor grade and clinical presentation (e.g., diagnostic vs theranostic settings) **(Table 2).**

Currently, it is recommended by all guidelines to use PET with somatostatin analogs radiolabeled with ^{68}Ga for somatostatin receptor targeting (collectively named SSTR-PET) rather than ^{99m}Tc- or ^{111}In-based somatostatin receptor scintigraphy in patients with known or suspected NEN. The value of SSTR PET, however, depends on the embryological origin of a NEN. SSTR PET can fail to detect insulinoma, hindgut NEN, thymic NEN, and MTC.[1] For diagnosis and (re)staging of well-differentiated (WD)-NEN, it is recommended to use SSTR PET as the first choice, except for insulinoma and MTC. It is also recommended in NEN patients with an unknown primary tumor, including ectopic Cushing syndrome. For small intestine (SI)-NENs, ^{68}Ga-SSA-PET/CT and ^{18}F-FDOPA should be considered as widely exchangeable for disease staging in most cases.[1,10-12] For insulinoma, GLP-1R imaging (^{68}Ga-exendin-4 PET preferred) is recommended as the first choice but it is only available in a few centers.[2] If not available, ^{68}Ga-SSA or carbidopa-assisted ^{18}F-FDOPA can be used as second choices. For MTC, ^{18}F-FDOPA is recommended as the first choice.[1,3,4,13] In the case of pheochromocytoma and paraganglioma, the genetic backgound must be considered when choosing the best radiophamaceutical: ^{68}Ga-SSA-PET/CT should be used for *SDHx*-mutated tumors, head and neck paraganglioma and metastatic cases, whereas ^{18}F-FDOPA should be used for adrenal pheochromocytoma (sporadic or related to *VHL, EPAS, RET, NF1,* and *MAX*-mutations).[5]

In a theranostic setting (Peptide Receptor Radionuclide Therapy: PPRT), ^{68}Ga-SSA is recommended as the first choice for PET imaging of NEN. ^{18}F-FDG should additionally be performed for a more comprehensive molecular imaging assessment and is mainly used as a prognostic biomarker for risk stratification. It has also shown great potential for predicting outcomes prior to PRRT.[14,15]

Regardless of the clinical presentation, images should be read by a physician who is both trained in PET/CT imaging and informed about the clinical context of the scan indication (e.g., staging, assessment for PRRT, or restaging). Personal medical history including existence of a known inherited disease, previous therapeutic interventions, and tumor grade must be considered for proper imaging interpretation.

Table 2. Value of specific radiopharmaceuticals according to tumor origin

	^{68}Ga-SSA	^{18}F-DOPA	Other specific tracers*
Pancreas Duodenum Gastrinoma Lung	+++	+/-	^{11}C-5-HTP (pNET)
Insulinoma	++	++ (very early[1], Carbidopa-assisted)	^{68}Ga-exendin-4 (GLP-1R)
Small intestine	+++	+++	^{11}C-5-HTP
Colon Rectum Thymus	++	+/-	
MTC	+/-	++ (early)	CCK-2 tracers
PHEO/PGL	+++[2]	+++[3]	^{18}F-fluorodopamine ^{18}F-meta-fluorobenzylguanidine

Clinical value: +/-= poor; +: moderate, ++= good; +++= very good
[1]Image acquisition should start immediately after tracer injection
[2]Extra-adrenal PGL (except *VHL, EPAS (HIF2A))*, metastatic pheochromocytoma and paraganglioma, head and neck paraganglioma
[3]Sporadic, *VHL, EPAS1 (HIF2A), MEN2, NF1, MAX*-related pheochromocytoma
5-HTPP: 5-Hydroxytryptophan
CCK-2= cholecystokinin (CCK) 2 receptor
*not available worldwide or under evaluation

Pitfalls and caveats on SSTR-PET

Physiologic biodistribution

Physiologic uptake is present in the kidneys, bladder, spleen, liver, pituitary, adrenal glands, salivary glands, and the thyroid. Uptake by the cervico-thoracic (stellate) sympathetic ganglia is frequently seen (unilateral or bilateral foci) and should not be misinterpreted as abnormal.[16] The stellate ganglia are ovalshaped structures located anterior to the neck of the first rib.

Focal tracer uptake that cannot be explained by physiologic biodistribution or that is higher than organ background activity should be considered pathological, especially if there is a correlated abnormality seen on CT.

Normal variants

An increased physiologic uptake in the head/uncinate process of the pancreas is commonly observed and is thought to be caused by a higher pancreatic polypeptide producing cell density in this region. There is a significant overlap between the uptake values of the physiologic pancreas and tumoral lesions of the head/uncinate process, which can result in false positive interpretations. Correlation with morphological imaging (MRI or multiphase CT) can be useful in challenging cases.

Congenital ectopic splenic nodules can be seen on SSTR PET. Accessory spleens (splenules) typically appear as round or oval nodules that are usually less than 2 cm in diameter. They are most commonly located near the lower third of postero-medial part of the spleen or near or in the pancreatic tail. Rarely, they may be located elsewhere in the abdomen. An intrapancreatic accessory spleen can be misdiagnosed as a pancreatic NEN. Differentiation between these anatomic variants from pathologic disorders (tumors in abdominal organs, lymphadenopathy, or peritoneal metastases) can be challenging. In these cases, heat-denatured red blood cell or sulfur colloid SPECT/CT may be useful to confirm the diagnosis of ectopic reticulo-endothelial tissue **(Table 3).**

Pancreatic heterotopia (PH) is a congenital anomaly defined as ectopic pancreatic tissue outside the normal pancreas. This displacement is most common in the stomach, duodenum, and proximal jejunum. This should be considered as a potential pitfall, even though it is rarely described on SSTR-PET.[17]

Pathological conditions

False positive findings

Splenosis, which is an acquired condition related to autotransplantation of splenic cells in the peritoneal cavity following splenic rupture or splenectomy, can also be visualized. As a result of limited blood supply, they are usually small in size and typically found adjacent to the small bowel serosa, the greater omentum, the parietal peritoneum, or the diaphragm **(Figure 1).** Again, scintigraphy of the reticuloendothelial system may be useful for accurate diagnosis in difficult cases.

Pancreatic serous cystadenoma can also exihibit an increased uptake on SSTR-PET.

Areas of high osteoblastic activity can have increased osseous uptake on SSTR-PET. These include degenerative changes, fractures, and benign lesions such as hemangioma **(Figure 1),** enchondroma, fibrous dysplasia. In challenging cases, review with correlative

morphological imaging with dedicated CT and/or MRI increases the reader's confidence in interpretation of SSTR-PET.

Inflammatory uptake can be seen in reactive hilar, mediastinal, axillary, or inguinal nodes. These are usually visualized in post-radiation therapy changes or any other inflammatory processes including sarcoidosis, tuberculosis and infections.

Meningioma are commonly incidentally discovered and appear as highly-avid extra-axial masses located over the cerebral convexity, in the parasagittal region, or arising from the sphenoid wing **(Table 3).**

Table 3. Summary of limitations and potential pitfalls in SSTR-PET interpretation

Potential false positives	Potential false negatives
Uncinate process	Low differentiated NEN
Stellate ganglia	Thymic NEN
Splenules (accessory spleens), splenosis	MTC
Pancreatic heterotopia	
Pancreatic serous cystadenoma	
Bone hemangioma, enchondroma, fibrous dysplasia	
Active chronic inflammation (e.g., sarcoidosis, tuberculosis, Hashimoto's thyroiditis)	
Other tumors (e.g., meningioma, breast cancer, renal cancer, lymphoma, thyroid neoplasms, glioma, neuroblastoma)	

False negative findings

Low differentiated NEN and MTC can be missed by SSTR-PET. Some insulinomas that do not express SSTR2 are not detected. In ectopic Cushings syndrome, the primary tumor may remain occult for a long period of time regardless of the imaging modality used.[18,19]

Caveats

NEN may occur in patients affected by an inherited tumor-predisposing syndrome **(Table 4).** In these patients, tumor uptake can be related to another primary NEN or other malignancies that should be distinguished from metastases. The distinction between neuroendocrine and other cancerous lesions can be difficult and may require biopsy for confirmation. For example, a biopsy may be warranted in cases of unexpected tumor growth in earlier diagnosed well-differentiated/low grade tumors or in the presence of dissociated progression during therapy.

Otherwise, the presence of tumors involving various organ systems should raise the possibility of a syndromic disease such as VHL or MEN1 disease. Multiple endocrine neoplasia type 1 (MEN1) is a hereditary syndrome predisposing a patient to parathyroid hyperplasia, which is the typically the first manifestation and is consistently observed. Other tumors associated with this syndrome include: pituitary adenoma, duodenopancreatic, thymic NEN, lung NEN, gastrinoma, and adrenocortical tumors. Duodenopancreatic (often multiple), thymic NEN, and lung NEN can be detected by SSTR-PET.[20,21] Von Hippel-Lindau *(*VHL*)* disease is a hereditary cancer syndrome caused by germline mutation of the *VHL* suppressor gene. Different *VHL* mutations confer different site-specific risks of cancer. Briefly, type 2

VHL mutations (missense) confer increased risk of PHEO with (type 2A: PHEO and hemangiobastoma, and 2B: PHEO and clear cell renal cell carcinoma (ccRCC) and hemangiobastoma) or without (type 2C: PHEO alone) stigmata of VHL disease. Both CNS hemangioblastoma or ccRCC can be detected on SSTR-PET.[22] *VHL*-related CNS hemangioblastoma can be multifocal and found in the cerebellum, brainstem, spinal cord or more rarely in the supratentorial region (**Figure 2)**. *VHL* patients may develop pancreatic tumors of various origin: cysts (simple, being more frequent than serous cystadenomas), NEN, solid microcystic serous adenoma, and pancreatic metastasis from ccRCC (**Figure 3)**. Pancreatic serous adenoma be mistaken for PNEN on morphological imaging and can also be positive on SSTR-PET[23] **(Table 4).**

Table 4. Inherited endocrine syndromes

	NEN	Non-NEN
MEN1	Pancreatic, thymic, lung NEN	Parathyroid hyperplasia, pituitary adenoma, adrenocortical adenoma
MEN2	Pheochromocytoma, medullary thyroid carcinoma	
VHL	Pheochromocytoma, paraganglioma, pancreatic NEN	CNS hemangioblastoma, ccRCC, pancreatic tumors/cysts, endolymphatic sac tumors, epididymal and broad ligament cysts
SDHx	Pheochromocytoma, paraganglioma, pituitary adenoma (3PAs)	GIST (Carney-Stratakis syndrome), ccRCC pulmonary chondroma

Pitfalls and caveats on ^{18}F-FDOPA PET

Physiologic biodistribution

^{18}F-FDOPA accumulation is visible in the renal and biliary excretory system. This distribution could represent a potential pitfall when considering focal ureteric or intrahepatic biliary activity mimicking lymph node involvement or metastasis. A specific uptake is seen in basal ganglia since ^{18}F-FDOPA is converted into ^{18}F-Fdopamine in the presynaptic neurons and released inside the nigrostriatal synaptic cleft where it binds post-synaptic dopamine receptors. There is also an uptake in the liver, adrenal glands, and pancreatic gland. There is a faint uptake in the oesophagus, bowel, myocardium, and peripheral muscles.[24] A focal area of increased uptake of ^{18}F-FDOPA is to be considered to be pathological, especially if there is a correlated abnormal structure observed on CT.

Normal variants

^{18}F-FDOPA uptake is often intense and prolonged in the pancreas and is related to the decarboxylation properties of zymogen granules. A more intense accumulation can be seen in the uncinate process (specific cases). Adrenal uptake can be intense and is variable across patients. A symmetric uptake by morphologically normal adrenals is normal. The use of carbidopa premedication, an efficient inhibitor of the peripheral aromatic amino acid decarboxylase (AADC), can inhibit normal pancreatic uptake while preserving tumor uptake [25,26].

Pathological conditions

False positive findings

^{18}F-FDOPA is more specific than SSTR-PET. Although AADC expression has been demonstrated in certain malignancies, there are only few anecdotal cases of this.

Few positive findings have been reported in a large series of NEN patients consisting of multiple myeloma, hepatocellular carcinoma, schwannoma and chondrosarcoma.[27] Intense tumor ^{18}F-FDOPA uptake has also been described in case reports of squamous cell carcinoma,[28] poorly differentiated adenocarcinoma,[29] thyroid neoplasms of follicular origin,[30] **(Figure 4)** prolactinoma,[31] and melanoma.[32] Melanoma case reports can be explained by the high AADC expression which is involved in melanin biosynthesis. Prolactinoma uptake is expected to be related to the release of ^{18}F-dopamine in the hypothalamo-hypophyseal blood vessels by the arcuate nucleus **(Figure 5).** Solid pseudopapillary neoplasms (SPN) of the exocrine pancreas can also cause a potential pitfall.[33,34] These tumors are more likely to affect women (at least 75% of cases) who are younger than 30 years. These tumors are typically round, well-demarcated, variable in size (average 6 cm) and contain solid and cystic areas with hemorrhage. They are characterized by an intense ^{18}F-FDOPA uptake which is currently unexplained and can be misdiagnosed as NEN **(Figure 6).** In doubtful situations, these two conditions can be distinguished by SSTR-PET which is positive for NEN and negative for SPN **(Table 5).**

False negative findings

^{18}F-FDOPA can be negative in thymic NEN, duodenal NEN,[35] and it can be negative in 20-30% of insulinoma cases (even after carbidopa premedication). In MTC patients with

persistently elevated serum CT values, long serum CT doubling time, and normal or low serum CEA levels, ^{18}F-FDOPA can either be negative or drastically underestimate the extent of the disease. In *SDHx*-mutated patients, ^{18}F-FDOPA can be suboptimal for detecting primary tumors and/or metastases.

Table 5. Summary of limitations and potential pitfalls in ^{18}F-FDOPA-PET interpretation

Potential false positives	Potential false negatives
Solid pseudopapillary tumor of the pancreas	Thymic or duodenal NEN
Thyroid neoplasm	*SDHx*-related metastatic paraganglioma of sympathetic origin
Pituitary adenoma	
Squamous cell carcinoma	
Poorly differentiated adenocarcinoma	
Melanoma	
Multiple myeloma	
Hepatocellular carcinoma	
Schwannoma	
Chondrosarcoma	

Caveats

Multiple endocrine neoplasia type 2 (MEN2) is an autosomal dominant syndrome caused by germline activating point mutations in the *RET* proto-oncogene. MEN2 is divided into 2 groups, depending on their clinical features: MEN2A (95% of MEN2, including the former subgroup of familial MTC) and MEN2B (5%). Detection of ^{18}F-FDOPA-avid adrenal masses in the setting of MTC staging/restaging or *vice versa* is pathognomonic of MEN2. PHEO and PGL are caused by inherited genetic mutations more than other NEN (in up to 40% of cases). Presence of tumor multifocality and/or extra-adrenal locations should raise the suspicion of inherited forms, related to germline mutations in one of the *SDH* subunit encoding genes (collectively called *SDHx*). Additionally, pituitary adenomas that overexpress D2 dopamine receptor (i.e., prolactin and GH-secreting adenoma) can be visualized on ^{18}F-FDOPA PET.[36] Their coexistence with PHEO and PGL can be observed in the so-called "3 P association, 3PAs" syndrome which is related to *SDHx* or *MAX* mutations **(Table 4).** Detection of pituitary adenoma in a patient with pancreatic NEN should raise the suspicion of MEN1 **(Figure 5)**.

Pitfalls and caveats on ^{18}F-FDG PET

Physiologic biodistribution

Intense physiologic uptake is present in the brain, kidney and urinary tract. The liver, spleen and bone marrow usually show homogenous and moderate uptake. ^{18}F-FDG uptake in the myocardium is variable in a fasting state and can be inhibited by fat-rich and low-carbohydrate diets. Muscles can be visualized in case of contracture or when intense muscle activity precedes the examination. The oral cavity, pharynx, stomach and digestive tract can exihibit diffuse and moderate ^{18}F-FDG uptake.

Normal variants

Physiologic ^{18}F-FDG thymic uptake can be seen in young patients. Brown adipose tissue (BAT) activation is not uncommon and more frequent in children than in adults. It is also more frequently encountered in cold weather and in patients with a low body mass index. It can be distributed in the subcutaneous and/or visceral brown fat. BAT activation is mainly related to stimulation of the sympathetic nerves that activate glucose transport by brown adipocytes via activation of β_3-adrenoceptors. BAT uptake has the potential for both masking and mimicking of nodal disease. Intense BAT uptake is seen in about 20% of patients with PHEO and PGL[37,38] **(Figure 7).** ^{18}F-FDG uptake in the ovaries may be found during menstruation and ovulation in pre-menopausal women, potentially mimicking ovarian metastases especially in patients with advanced disease. Increased ^{18}F-FDG uptake in bone marrow and splenic activity is demonstrated after injection of granulocytic growth factors, as well as in patients with infection, inflammation, anemia, and those who recently received chemotherapy. Both clinical context and coregistration with CT slices can help overcome potential pitfalls.[39]

Pathological conditions

False positive findings

False ^{18}F-FDG findings can be related to inflammatory processes induced by surgery, radiotherapy, and recent or ongoing infection. The occurrence of another primary malignancy can be incidentally found in NEN patients and should be distinguished from metastases. In this setting, information about staging, grade and previous imaging studies can help make an accurate diagnosis.

False negative findings

False negative findings can be related to the indolent tumor behavior of most NENs such as G1 and low G2 NEN (Ki-67<5%),[14] MTC, sporadic PHEO/PGL, and insulinoma. Beyond this situation, tumor detection can also been masked in certain locations by unfavorable tracer biodistribution. For instance, in cases of intravesical or paravesical PGL. Nuclear physicians should be aware of this pitfall regardless of the tracer, especially in the evaluation of *SDHB* or *SDHD*-mutated patients. Thresholding and the use of diuretics may also help to circumvent this drawback **(Figure 8).**

Caveats

Gastrointestinal stromal tumors (GIST) can be rarely associated with PGL in patients with Carney triad and Carney–Stratakis syndrome. Carney triad is characterized by synchronous or metachronous occuring gastric GIST (always multiple), pulmonary chondroma, and PGL (mostly sympathetic-derived) **(Figure 9).** This condition is most common among young females and it is almost never inherited (due to epigenetic changes). By contrast, Carney-Stratakis syndrome (Carney dyad) comprises GIST and PGL, and it is related to germline mutations in one of the *SDH* genes.

Conclusion

Molecular imaging has gained an important role in NEN patients for diagnosis, staging/restaging, and disease phenotyping. It should be interpreted by a nuclear physician who is experienced in NEN and considerate of possible pitfalls, variants, and caveats.

References

1. Bozkurt MF, Virgolini I, Balogova S, et al. Guideline for PET/CT imaging of neuroendocrine neoplasms with (68)Ga-DOTA-conjugated somatostatin receptor targeting peptides and (18)F-DOPA. *Eur J Nucl Med Mol Imaging* 2017; **44**(9): 1588-601.
2. Falconi M, Eriksson B, Kaltsas G, et al. ENETS Consensus Guidelines Update for the Management of Patients with Functional Pancreatic Neuroendocrine Tumors and Non-Functional Pancreatic Neuroendocrine Tumors. *Neuroendocrinology* 2016; **103**(2): 153-71.
3. Filetti S, Durante C, Hartl D, et al. Thyroid cancer: ESMO Clinical Practice Guidelines for diagnosis, treatment and follow-updagger. *Ann Oncol* 2019; **30**(12): 1856-83.
4. Giovanella L, Treglia G, Iakovou I, Mihailovic J, Verburg FA, Luster M. EANM practice guideline for PET/CT imaging in medullary thyroid carcinoma. *Eur J Nucl Med Mol Imaging* 2020; **47**(1): 61-77.
5. Taieb D, Hicks RJ, Hindie E, et al. European Association of Nuclear Medicine Practice Guideline/Society of Nuclear Medicine and Molecular Imaging Procedure Standard 2019 for radionuclide imaging of phaeochromocytoma and paraganglioma. *Eur J Nucl Med Mol Imaging* 2019; **46**(10): 2112-37.
6. Sundin A, Arnold R, Baudin E, et al. ENETS Consensus Guidelines for the Standards of Care in Neuroendocrine Tumors: Radiological, Nuclear Medicine & Hybrid Imaging. *Neuroendocrinology* 2017; **105**(3): 212-44.
7. Hope TA, Bergsland EK, Bozkurt MF, et al. Appropriate Use Criteria for Somatostatin Receptor PET Imaging in Neuroendocrine Tumors. *J Nucl Med* 2018; **59**(1): 66-74.
8. Howe JR, Cardona K, Fraker DL, et al. The Surgical Management of Small Bowel Neuroendocrine Tumors: Consensus Guidelines of the North American Neuroendocrine Tumor Society. *Pancreas* 2017; **46**(6): 715-31.
9. Ambrosini V, Kunikowska J, Baudin E, et al. Consensus on molecular imaging and theranostics in neuroendocrine neoplasms. *Eur J Cancer* 2021; **146**: 56-73.
10. Ouvrard E, Chevalier E, Addeo P, et al. Intraindividual comparison of (18) F-FDOPA and (68) Ga-DOTATOC PET/CT detection rate for metastatic assessment in patients with ileal neuroendocrine tumours. *Clin Endocrinol (Oxf)* 2021; **94**(1): 66-73.
11. Ansquer C, Touchefeu Y, Faivre-Chauvet A, et al. Head-to-Head Comparison of 18F-DOPA PET/CT and 68Ga-DOTANOC PET/CT in Patients With Midgut Neuroendocrine Tumors. *Clin Nucl Med* 2021; **46**(3): 181-6.
12. Veenstra EB, de Groot DJA, Brouwers AH, Walenkamp AME, Noordzij W. Comparison of 18F-DOPA Versus 68Ga-DOTATOC as Preferred PET Imaging Tracer in Well-Differentiated Neuroendocrine Neoplasms. *Clin Nucl Med* 2021; **46**(3): 195-200.
13. Castinetti F, Taieb D. Positron Emission Tomography Imaging in Medullary Thyroid Carcinoma: Time for Reappraisal? *Thyroid* 2020.
14. Binderup T, Knigge U, Johnbeck CB, et al. (18)F-FDG-PET is superior to WHO grading as prognostic tool in neuroendocrine neoplasms and useful in guiding peptide receptor radionuclide therapy: a prospective 10-year follow-up study of 166 patients. *J Nucl Med* 2020.
15. Zhang J, Liu Q, Singh A, Schuchardt C, Kulkarni HR, Baum RP. Prognostic Value of (18)F-FDG PET/CT in a Large Cohort of Patients with Advanced Metastatic Neuroendocrine Neoplasms Treated with Peptide Receptor Radionuclide Therapy. *J Nucl Med* 2020; **61**(11): 1560-9.
16. Berg Z, Koppula BR. 68Ga-DOTATATE Uptake by Cervicothoracic (Stellate) Ganglia. *Clin Nucl Med* 2019; **44**(10): 810-1.

17. Zilli A, Fanetti I, Conte D, Massironi S. A case of positive (68)Ga-DOTATOC-PET/CT pancreatic heterotopia mimicking an intestinal neuroendocrine tumor. *Clin Imaging* 2018; **49**: 156-8.
18. Isidori AM, Sbardella E, Zatelli MC, et al. Conventional and Nuclear Medicine Imaging in Ectopic Cushing's Syndrome: A Systematic Review. *J Clin Endocrinol Metab* 2015; **100**(9): 3231-44.
19. Wannachalee T, Turcu AF, Bancos I, et al. The Clinical Impact of [(68) Ga]-DOTATATE PET/CT for the Diagnosis and Management of Ectopic Adrenocorticotropic Hormone - Secreting Tumours. *Clin Endocrinol (Oxf)* 2019; **91**(2): 288-94.
20. Morgat C, Velayoudom-Cephise FL, Schwartz P, et al. Evaluation of (68)Ga-DOTA-TOC PET/CT for the detection of duodenopancreatic neuroendocrine tumors in patients with MEN1. *Eur J Nucl Med Mol Imaging* 2016; **43**(7): 1258-66.
21. Lastoria S, Marciello F, Faggiano A, et al. Role of (68)Ga-DOTATATE PET/CT in patients with multiple endocrine neoplasia type 1 (MEN1). *Endocrine* 2016; **52**(3): 488-94.
22. Shell J, Tirosh A, Millo C, et al. The utility of (68)Gallium-DOTATATE PET/CT in the detection of von Hippel-Lindau disease associated tumors. *Eur J Radiol* 2019; **112**: 130-5.
23. Nappo G, Funel N, Giudici S, et al. Pancreatic serous cystoadenoma (CSA) showing increased tracer uptake at 68-GaDOTA-peptide Positron Emission Tomography (68Ga-DOTA-peptide PET-CT): a case report. *BMC Surg* 2020; **20**(1): 331.
24. Chondrogiannis S, Marzola MC, Al-Nahhas A, et al. Normal biodistribution pattern and physiologic variants of 18F-DOPA PET imaging. *Nucl Med Commun* 2013; **34**(12): 1141-9.
25. Imperiale A, Sebag F, Vix M, et al. 18F-FDOPA PET/CT imaging of insulinoma revisited. *Eur J Nucl Med Mol Imaging* 2015; **42**(3): 409-18.
26. Leroy-Freschini B, Amodru V, Addeo P, et al. Early (18)F-FDOPA PET/CT imaging after carbidopa premedication as a valuable diagnostic option in patients with insulinoma. *Eur J Nucl Med Mol Imaging* 2019; **46**(3): 686-95.
27. Berends AMA, Kerstens MN, Bolt JW, et al. False-positive findings on 6-[18F]fluor-l-3,4-dihydroxyphenylalanine PET ((18)F-FDOPA-PET) performed for imaging of neuroendocrine tumors. *Eur J Endocrinol* 2018; **179**(2): 125-33.
28. Dietemann S, Debry C, Onea A, Namer IJ, Imperiale A. Epiglottic Squamous Cell Carcinoma Showing Unexpected 18F-FDOPA Uptake on PET/CT Investigation. *Clin Nucl Med* 2015; **40**(7): e370-1.
29. Heimburger C, Averous G, Charlin E, Lang H, Kurtz JE, Imperiale A. Adrenal Metastasis of a Poorly Differentiated Adenocarcinoma Mimicking a Pheochromocytoma on 18F-FDOPA PET/CT. *Clin Nucl Med* 2016; **41**(9): 691-2.
30. Pauleau G, Palazzo FF, Essamet W, Sebag F, Taieb D. Hurthle cell neoplasms: a new differential diagnosis for 18F-FDOPA-avid thyroid nodules? *J Clin Endocrinol Metab* 2013; **98**(3): 865-6.
31. Ginet M, Cuny T, Schmitt E, Marie PY, Verger A. 18F-FDOPA PET Imaging in Prolactinoma. *Clin Nucl Med* 2017; **42**(8): e383-e4.
32. Zhang-Yin J, Jublanc C, Aouidad I, Montravers F, Talbot JN. Incidental Metastatic Melanoma Identified on 18F-FDOPA PET/CT With Confirmation by Histology. *Clin Nucl Med* 2020; **45**(10): 817-8.
33. Imperiale A, Addeo P, Averous G, Namer IJ, Bachellier P. Solid pseudopapillary pancreatic tumor mimicking a neuroendocrine neoplasm on (1)(8)F-FDOPA PET/CT. *J Clin Endocrinol Metab* 2013; **98**(7): 2643-4.
34. Somme F, Montaz-Rosset MS, Averous G, et al. Solid pseudopapillary tumour should be part of differential diagnosis of focal pancreatic lesions with increased (18) F-FDOPA uptake. *Clin Endocrinol (Oxf)* 2020; **93**(1): 78-81.

35. Imperiale A, Averous G, Helali M, et al. Limited role of carbidopa-assisted (18)F-FDOPA PET/CT in patients with sporadic non-functional gastroduodenal neuroendocrine neoplasms. *Ann Nucl Med* 2019; **33**(9): 697-707.
36. Heimburger C, Bund C, Addeo P, Goichot B, Imperiale A. 18F-FDOPA Uptake Reflects the Efficacy of Dopamine Agonists Treatment in Pituitary Prolactinoma. *Clin Nucl Med* 2018; **43**(9): e324-e5.
37. Abdul Sater Z, Jha A, Hamimi A, et al. Pheochromocytoma and Paraganglioma Patients With Poor Survival Often Show Brown Adipose Tissue Activation. *J Clin Endocrinol Metab* 2020; **105**(4).
38. Puar T, van Berkel A, Gotthardt M, et al. Genotype-Dependent Brown Adipose Tissue Activation in Patients With Pheochromocytoma and Paraganglioma. *J Clin Endocrinol Metab* 2016; **101**(1): 224-32.
39. Boellaard R, Delgado-Bolton R, Oyen WJ, et al. FDG PET/CT: EANM procedure guidelines for tumour imaging: version 2.0. *Eur J Nucl Med Mol Imaging* 2015; **42**(2): 328-54.

Figure legends

Figure 1. Splenosis and vertebral hemangioma in a NEN patient
A 67-year-woman followed by imaging for a pancreatic NEN. SSTR PET/CT showed multiple mesenteric splenosis nodules (A, B, short arrows) and a bone uptake centered over the transverse process of T7 (long arrows) (D, F). Sulfur colloid SPECT/CT confirmed the diagnosis of splenosis (not shown). Axial T1 spin echo (C), T2 spin echo (E) and post-gadolinium fat-saturated T1 MR images (F) demonstrated a vertebral hemangioma involving the right pedicle and transverse process of T7 with the typical polka-dot sign (circle) and adjacent soft tissue extension (arrowheads) both in the epidural fat and perivertebral tissue.

Figure 2. Hemangioblastoma in a *VHL* patient
A 23-year-old man with VHL disease was evaluated by SSTR PET/CT for follow-up. His father had PHEO and CNS hemangioblastoma. He had a bilateral PHEO with history of right total adrenalectomy. SSTR PET/CT showed an uptake foci located at the L5/S1 spinal level (A: MIP, B: axial PET/CT, arrows), in addition to the left PHEO (C: axial PET/CT, short arrow). MRI showed an intensely and homogeneously enhancing 6 mm nodule of the cauda equina which was consistent with the diagnosis of hemangioblastoma.

Figure 3. RCC metastasis and hemangioblastoma in a *VHL* patient
A 75-year-old man with VHL disease and previous history of ccRCC operated 22 years ago. In 2020, the patient was referred for a kinetic cerebellar syndrome. The imaging work-up revealed 4 hypervascular pancreatic lesions suspected of NET origin (3, 9, 13, and 34 mm), a 8 mm lung (left laterobasal) nodule, and lesions of the posterior cerebral fossa (A). The patient underwent in-bloc resection of a 2 cm lesion located in the right cerebellar tonsil. The final diagnosis corresponded to a hemangioblastoma. SSTR PET/CT showed a left medial sphenoid meningioma (B, arrow), two small foci in the right cerebellum (C, arrows), a left inferior lung nodule (D, arrow), and 3 pancreatic lesions. The largest pancreatic lesion (E, arrow) was biopsied and revealed a pancreatic metastasis from a RCC origin.

Figure 4. Thyroid adenoma incidentally found in a *SDHB* mutated patient
A 42-year-old woman with *SDHB* mutation underwent ^{18}F-FDOPA PET/CT (A: anterior PET MIP; B, D: axial PET/CT) for disease staging. ^{18}F-FDOPA PET/CT showed a left vagal paraganglioma (arrowhead) and two intense thyroid uptake foci (arrows). Neck ultrasonography was concordant with PET findings and showed two isoechoic nodules with peripheral vascular signal (E). Pathological analysis after right thyroidectomy, and US-guided fine-needle aspiration cytology showed benign features (C).

Figure 5. Prolactinoma in a *MEN1* patient
A 35-year-old woman was evaluated for MEN1 disease. ^{18}F-FDOPA PET/CT showed a focal pituitary uptake (A: lateral MIP, B: sagittal PET, C: sagittal PET/CT, arrows). Pituitary MRI revealed a right pituitary microadenoma (10 x 6 mm) (D). These findings together with elevated serum prolactin (1920 mUI/l) were consistent with the diagnosis of prolactinoma.

Figure 6. Solid pseudopapillary neoplasm
A 32-year-old woman with a 6 cm cystic mass of the pancreatic tail (contrast-enhanced CT (A) and MRI (D), arterial phase, asterix) was evaluated by ^{18}F-FDOPA. ^{18}F-FDOPA PET/CT showed an intense ^{18}F-FDOPA tumor uptake (C, F: PET, PET/CT axial slice) while SSTR PET was negative (B, E: PET, PET/CT axial slice). The diagnosis of solid pseudopapillary neoplasm was pathologically confirmed.

Figure 7. BAT activation related in a pheochromocytoma patient
A 61-year-old man presented with headaches, palpitations, a 7 cm adrenal mass, and highly elevated normetanephrine values was evaluated by ^{18}F-FDG PET/CT (**A, B**: anterior and lateral MIP projections, **C-F**: coronal, sagittal, and axial PET/CT). ^{18}F-FDG PET/CT showed the pheochromocytoma (arrows) and demonstrated an intense adrenal brown adipose tissue activation (BAT) related to norepinephrine hypersecretion. The pheochromocytoma was removed and genetic screening was negative. Post-operative ^{18}F-FDG PET/CT was normal without BAT uptake (not shown).

Figure 8. *SDHB*-related vesical paraganglioma masked by tracer accumulation in urinary bladder
A 13-year-old child with germline *SDHB* mutation was evaluated by ^{18}F-FDG PET/CT for disease restaging. MRI revealed a 30 mm solid hypervascular lesion along the left external iliac artery in intimate contact with the bladder wall (A, arrow). ^{18}F-FDG PET/CT images were blindly evaluated to the MRI results and initially interpreted as normal (B, C). Nonetheless, after adjusting the image contrast and thresholding, a pathological focal uptake (D, E, F, arrows) was detected corresponding to the pelvic tumor shown by MRI. After resection, the diagnosis of paraganglioma was pathologically confirmed.

Figure 9. GIST occurring in the setting of Carney triad
A 19-year-old woman was evaluated for suspicion of thoracic paraganglioma located in the right costovertebral angle of T2. ^{18}F-FDOPA PET/CT confirmed the diagnosis and revealed an additional tiny abdominal paraaortic paraganglioma (A, short arrows). ^{18}F-FDG PET/CT missed the abdominal paraganglioma. Despite intense activity of abdominal brown adipose tissue (due to norepinephrine secretion), ^{18}F-FDG PET/CT found an avid lower gastric mass raising suspicion of a gastric tumor (arrows). There was also bone marrow activation noted. Esophagogastroduodenoscopy showed a 4.0 cm polypoidalal mass along the lesser curvature of the antrum with exophytic growth and superficial mucosal ulceration. The biopsy confirmed the diagnosis of GIST. The patient underwent gastric surgery with findings consistent with multiple GIST.

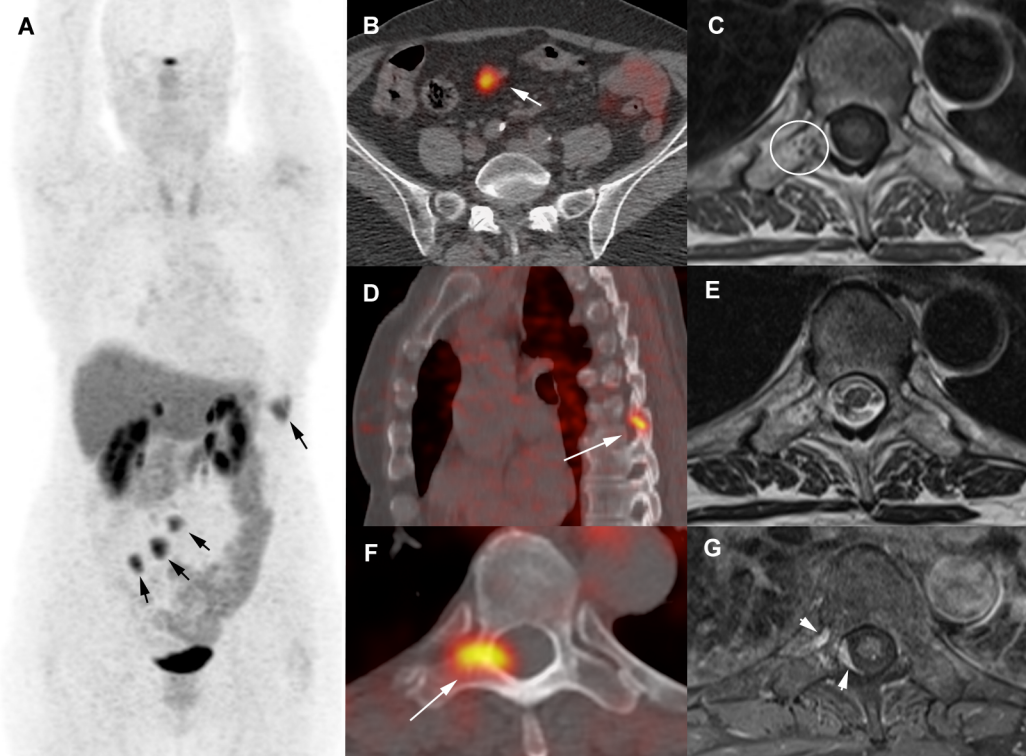
A
B
C
D
E
F
G


A
B
C

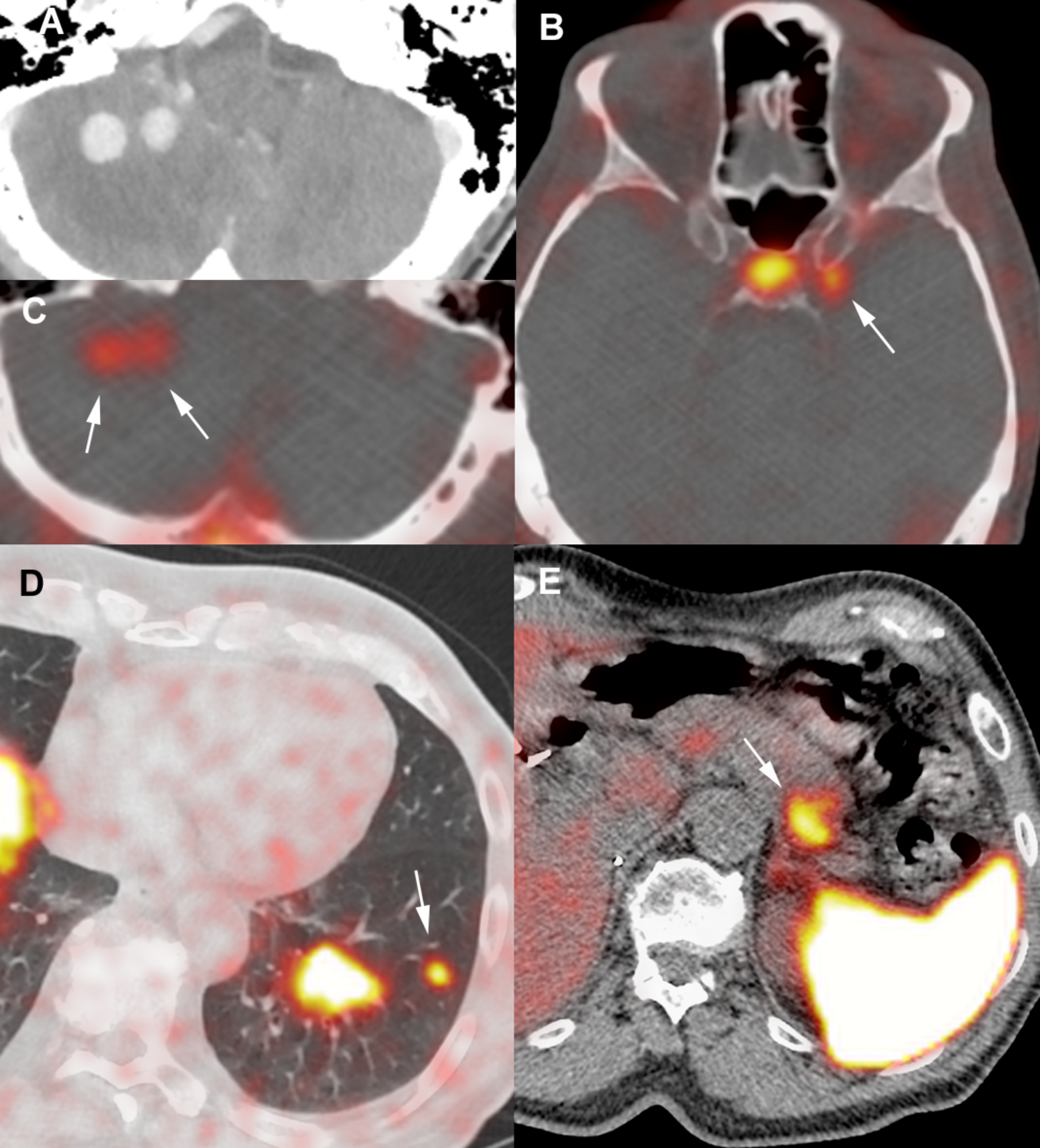
A
B
C
D
E

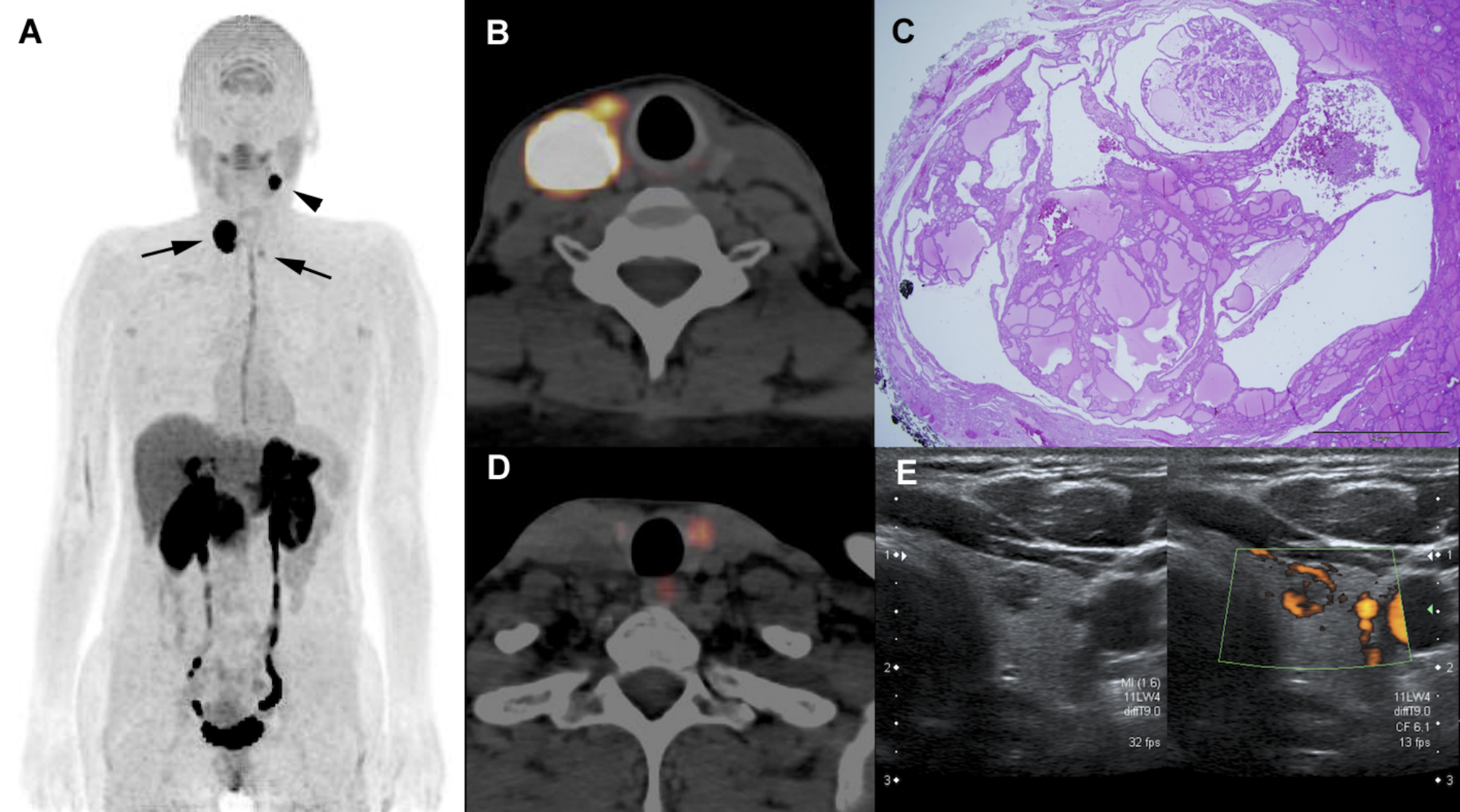
A
B
C
D
E
MI (1.6)
11LW4
diffT9.0
32 fps
11LW4
diffT9.0
CF 6.1
13 fps

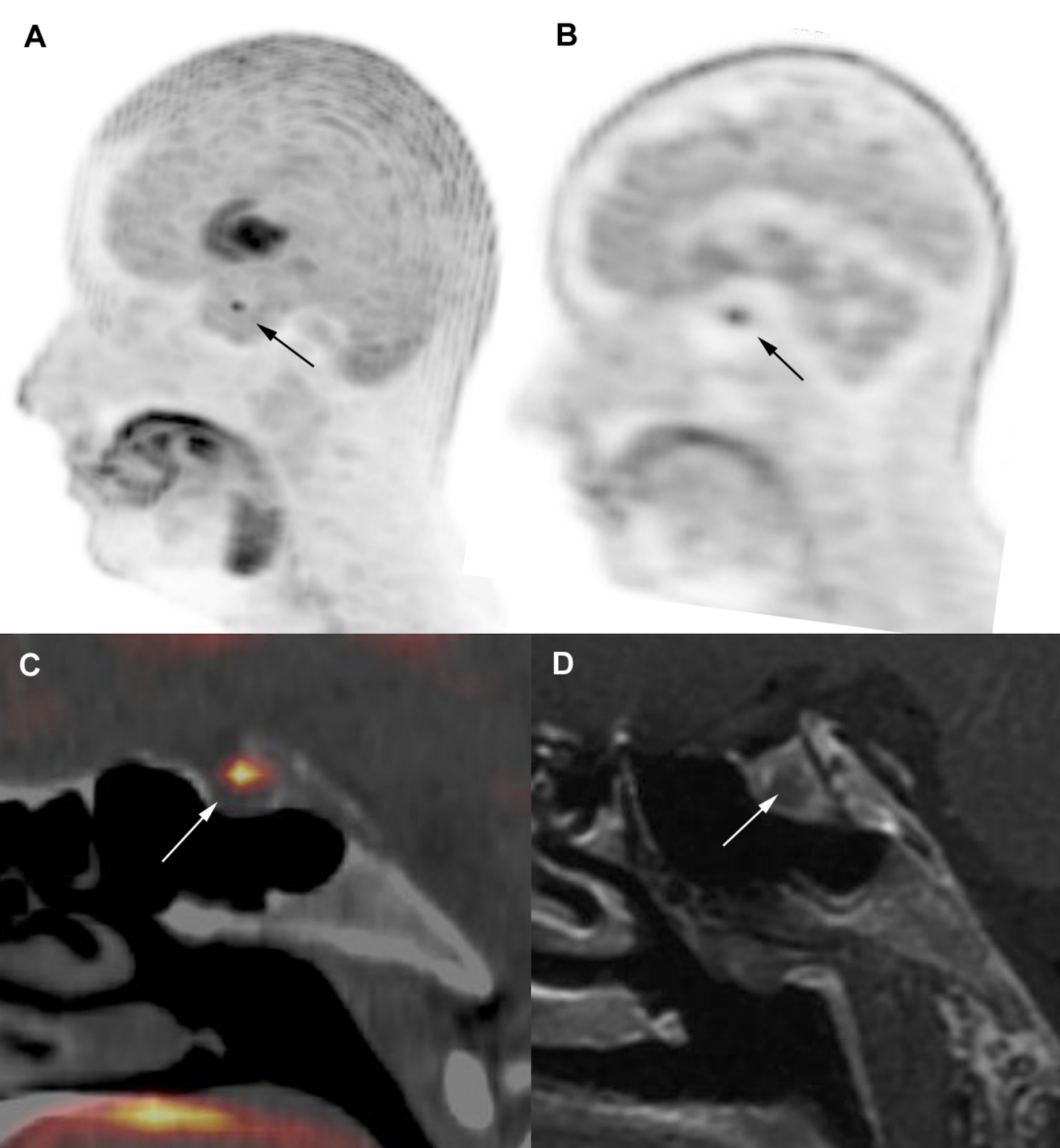
A
B
C
D

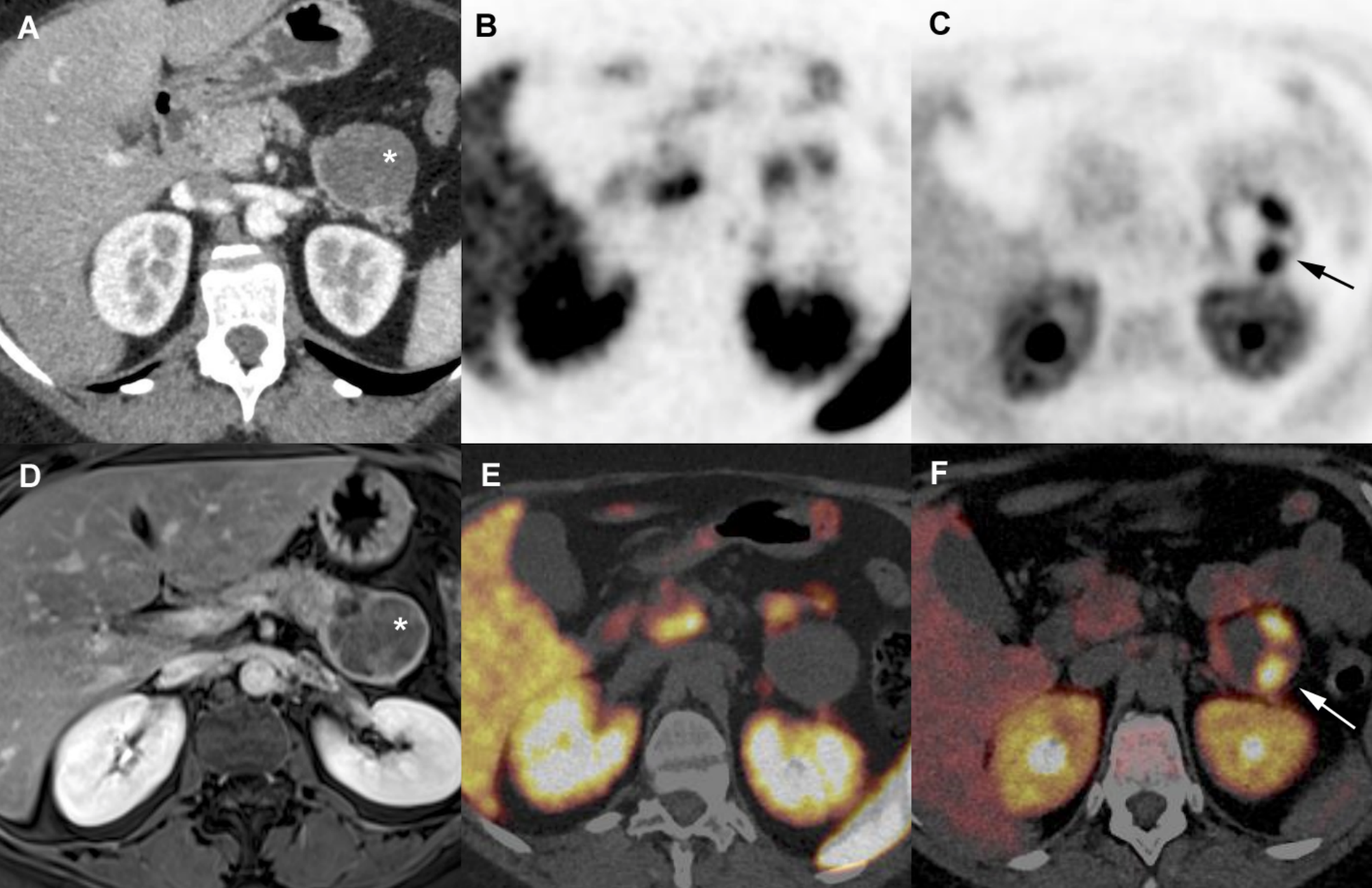
A
B
C
D
E
F

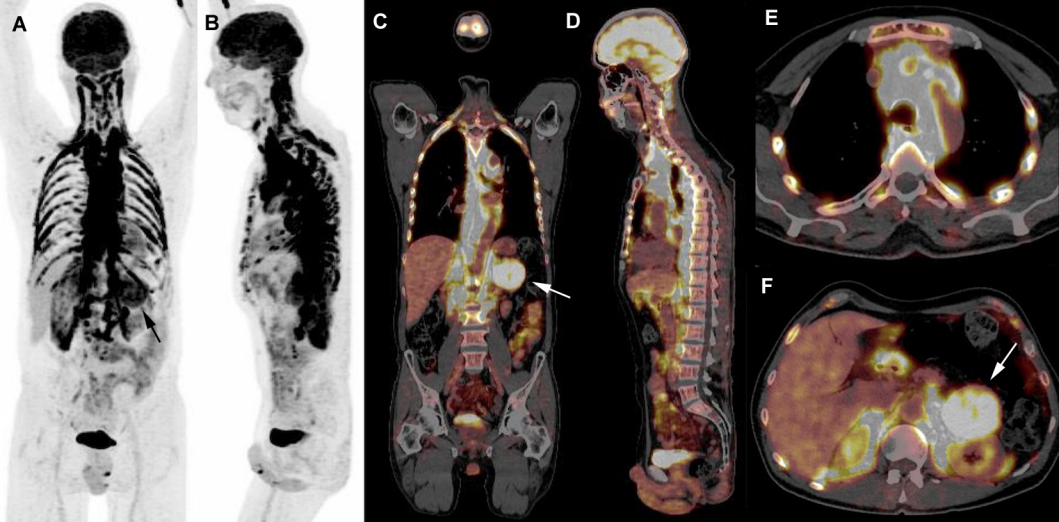
A
B
C
D
E
F

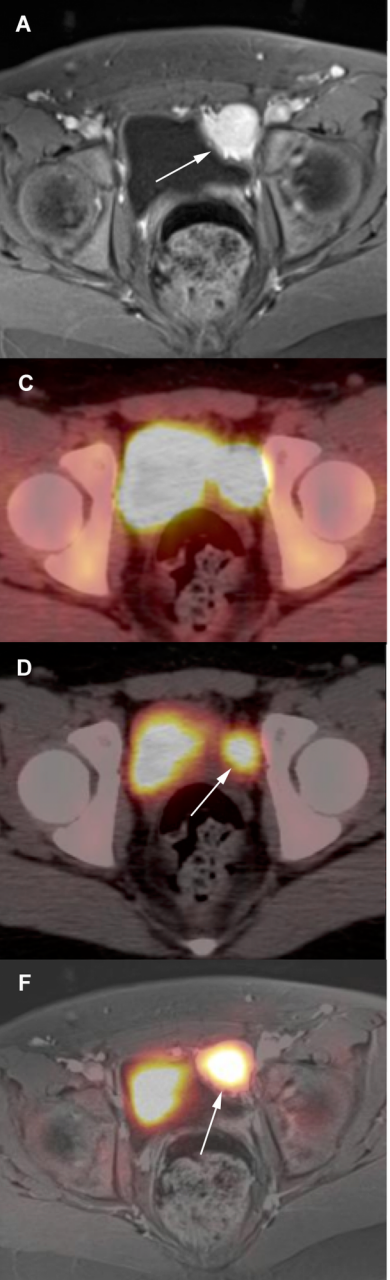
A
B
C
D
E
F

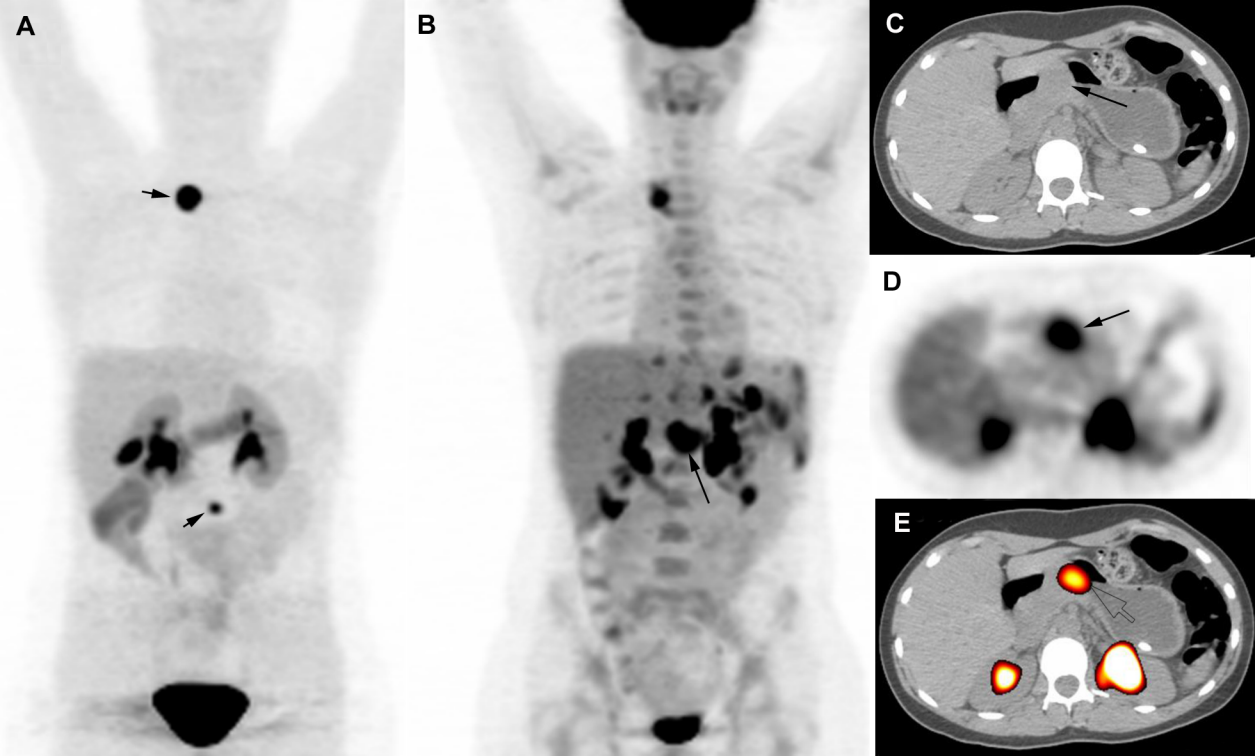
A
B
C
D
E